Metal-carbon hybrid multijunction electronic devices

Neeraj Dwivedi[a,b,1,2], Sushil Kumar[a,*], J. David Carey[c,d] and Hitendra K. Malik[b]

[a] *National Physical Laboratory (CSIR), K.S. Krishnan Road, New Delhi – 110 012, India,*

[b] *Department of Physics, Indian Institute of Technology Delhi, New Delhi – 110 016, India,*

[c] *Advanced Technology Institute, University of Surrey, Guildford, GU2 7XH, Surrey, United Kingdom*

[d] *Department of Electronic Engineering, University of Surrey, Guildford, GU2 7XH, Surrey, United Kingdom*

Abstract

Understanding the factors that influence the structural, mechanical and electrical properties of hybrid metal–carbon multilayer materials and devices are explored in this study by examining the effects of the choice of metal, Cu or Ti, and the number of metal-carbon bilayers. With up to four bilayers, corresponding to ten discrete metal-carbon electrical junctions, lower interfacial stresses and lower electrical resistance are always found in Cu multilayer structures, when compared with Ti containing multilayers. The lower electrical resistance is as a result of a copper-carbon interaction which facilitates a carbon sp^3 to sp^2 bonding transformation and is accompanied by a metal-induced transformation of the carbon layer from an amorphous to nanostructured morphology which also aids in conduction. Time-of-flight secondary ion mass spectrometry measurements demonstrate that the two selected metals, Cu and Ti, represent extreme examples in their affinity to bond with carbon with Cu (Ti) representing a weak (strong) affinity metal for bonding. This study shows the importance of the metal-carbon interaction in understanding the mechanical stresses and electrical characteristics in particular, and the wider result of the role played by the relative chemical reactivity of the components in multijunction hybrid semiconductor-based devices in general.

Keywords: carbon electronic devices, metal-carbon interaction, amorphous carbon, nanostructured carbon, hybrid electronic devices, heterojunctions, electrical properties

*Corresponding Author Tel.: +91-11-45608650, Fax: +91-11-45609310. Email address: skumar@nplindia.org (Sushil Kumar).

[1] Email: neerajdwivedi6@gmail.com (Neeraj Dwivedi)

[2]Present Address: Department of Electrical and Computer Engineering, National University of Singapore, Singapore

1. Introduction

Carbon based multilayer structures span the range from semi-metallic graphene-hBN based tunnelling devices [1], graphene and carbon nanotube devices for flexible and transparent electronics [2] to mixed sp^2 and sp^3 amorphous materials. Metal - diamond-like carbon (DLC) hybrid thin film structures have been shown that they can be used for stretchable electronics by employing gold [3], and the inclusion of tungsten is known to improve their mechanical properties, friction and reduce wear [4]. Amorphous carbon (a-C) thin films, and their hydrogenated form, a-C:H, have several advantages over other carbon based materials, such as graphene, nanotubes or diamond, as their intrinsic mechanical and electrical properties can be readily changed by varying the deposition conditions [5,6] without the need for post-deposition chemical surface functionalization and/or material processing. Thin film deposition on substrates, such as silicon or close-packed metals, can affect the amount of interfacial stress and influence the overall electrical transport properties. For example, Godet *et al.* [7] have developed descriptions of the transport mechanisms through a-C:H and modified a-C:H films, and more recently, the electronic conductivity of a-C:H thin films can be increased through the various inclusion of Ni-Cr dots [8] and via the inclusion of nitrogen dopant atoms [9]. Furthermore, in the area of high field electrical transport, we have previously been able to reduce the threshold electric field for the onset of cold electron emission from DLC films by nanostructuring the surface [10] using a combination of silver micron-sized dots with nitrogen incorporation [11], and alternatively, by employing a copper metal interlayer [12]. When in direct contact with a metal, a-C films have also shown a metal-insulator (M-I) transition [13,14] in which the metal-amorphous carbon structure can be efficiently used for switching applications opening up the possibility of use as memory storage devices.

Most electrical transport studies of a-C based materials to date have concentrated on single junction based a-C or a-C:H devices. For example, Miyajima *et al.* [15] have examined single a-

C/*n*-Si heterojunction devices and Hao *et al.* [16] have fabricated *p*-C/*n*-Si and Fe-C/*n*-Si heterostructure devices. These latter studies have employed single metal layers; what is unknown is how both the interfacial stress and conduction properties change in metal-carbon multilayer device architectures. Multiple electrical junctions, where metal and semiconducting/insulating layers are alternatively used, represent an attractive alternative to single junction devices and are routinely used, for example, in tandem solar cells. Such metal-insulator based multiple junction hybrid devices may demonstrate improved electrical characteristics, such as increases in conductivity, without the need of complex ultrathin layers, and in the case of large area carbon based materials may be readily produced using conventional commercial chemical vapor deposition (CVD) systems. In the present study, we investigate the mechanical interfacial stress and electrical transport characteristics of metal/a-C:H device multilayer structures by choosing the two metals, copper and titanium. We explore how increasing the number of alternating metal and a-C:H layers influences the electrical conduction in multijunction devices and demonstrate how the introduction of even a single metal layer increases the conductivity of a-C:H based devices. Amorphous carbon films are also known to usually have high intrinsic stress; while the addition of hydrogen lowers this stress it is often accompanied by an increased sp^3 fraction, with the net effect of an overall lower conductivity. The insertion of thin metal layers helps to lower the overall stress in the film without the need for increased H content and can result in improvements to the overall hybrid structure conductivity and film adhesion. The manuscript shows that the choice of metal plays an important role with differing behaviour between carbide and non-carbide forming metals. Copper, as a representative non-carbide metal, results in lower measured film stress with better adhesion and increased conductivity when compared to Ti, which is a carbide forming metal.

2. Experimental details

Multilayer films of Cu/a-C:H (Ti/a-C:H) were grown in an alternate sequence of Cu and a-C:H (Ti and a-C:H) layers on well-cleaned *n*-type silicon wafers, as well as on Corning 7059 glass substrates for optical characterization. Deposition occurred at a base pressure of 10^{-3} Torr in a

hybrid system combining radio-frequency plasma enhanced chemical vapor deposition (RF-PECVD) and RF-sputtering techniques. High purity Cu or Ti disks of 50 mm diameter were used as sputtering targets and the target to substrate distance was kept about 6 cm. The metal layers in the multilayer structures were deposited by sputtering at a constant negative self-bias of 300 V in an Ar atmosphere of 70 mTorr pressure. The a-C:H layers were deposited by PECVD on successive metal layers at a constant negative self-bias of 100 V in an atmosphere of C_2H_2 at 28 mTorr. The number of Cu/a-C:H (Ti/a-C:H) bilayers was varied from one to four, where a combination of one Cu (Ti) and one a-C:H layer forms a Cu (Ti)/a-C:H bilayer. Samples C-1, C-2, C-3 and C-4 (T-1, T-2, T-3 and T-4) were prepared using 1, 2, 3 and 4 bilayers of Cu/a-C:H (Ti/a-C:H), respectively, on *n*-Si wafers. Samples C-1G, C-2G, C-3G and C-4G (T-1G, T-2G, T-3G and T-4G) were prepared using 1, 2, 3 and 4 bilayers of Cu/a-C:H (Ti/a-C:H), respectively, on glass substrates [17]. The total thickness of the Cu/Ti and DLC layers of samples C-1, C-2, C-3 and C-4 (T-1, T-2, T-3 and T-4) was measured to be 56, 105, 154 and 205 nm, respectively (227, 277, 312 and 364 nm, respectively). The thickness of the Cu layers and Ti layers was kept at around 15 nm and around 20 nm, respectively. The thickness of each DLC layer was between 36 and 41 nm for the Cu/DLC films. However, the thickness of the first DLC layer for Ti/DLC films was kept at around 207 nm (sample T-1 possessed DLC thickness ~ 207 nm); the thickness of the second, third and fourth DLC layers was varied between 23 and 30 nm.

The residual stress of these multilayer samples was estimated using the change in radius of curvature method by a 500TC temperature controlled film stress measurement system (FSM Frontier Semiconductor, USA). The depth profile of these multilayer samples was analysed by time-of-flight secondary ion mass spectrometry (TOF-SIMS) from ION-TOF GmBH, Germany. For analysis, secondary ions were generated by bombarding pulsed primary ions from a Bi^+ liquid metal ion gun. The overall depth resolution during TOF-SIMS analysis was estimated to be 1 nm. The electrical contacts were made in a sandwich device configuration with Al, produced by thermal evaporation, serving as the top and bottom electrodes. Current-voltage (I-V) characteristics were recorded by varying the voltage from 0 to 10 V using a Keithley 4200 instrument. Structural information was found scanning electron microscopy. Figure 1 shows a

schematic of the Cu/a-C:H and Ti/a-C:H devices grown on a Si substrate with Al as electrodes. Since Cu/a-C:H and Ti/a-C:H multilayer structures have several metallic Cu and Ti interlayers, they generate several serially connected local junctions between the two electrodes. As shown schematically in Figure 1, metal-semiconductor-metal (MSM) structures, metal-insulator-metal (MIM) structures, metal-semiconductor (M-S) junction, and M-I junction with several junctions, are present. Device C-1, C-2, C-3 and C-4 (T-1, T-2, T-3 and T-4) possess a total number of 4, 6, 8 and 10 electrical junctions, respectively, as summarised in Table 1.

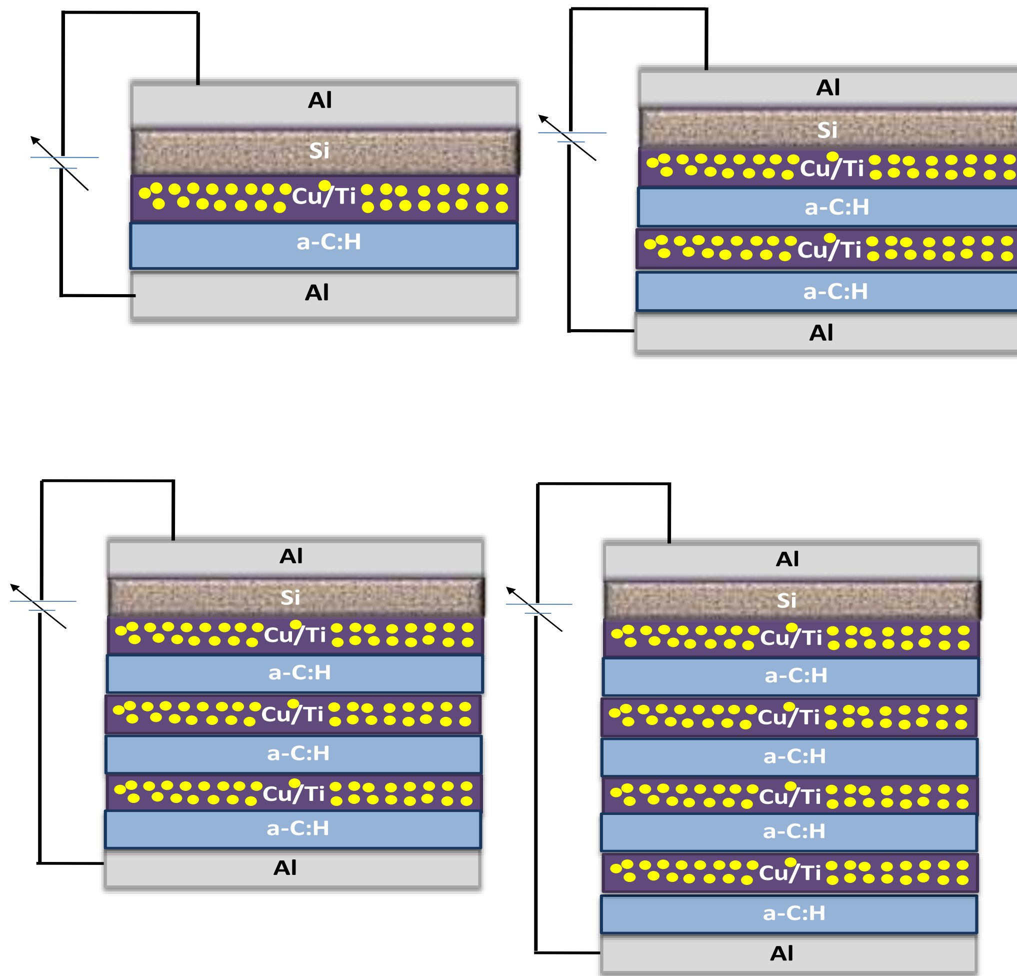

Figure 1: Schematic representation of hybrid Cu/a-C:H and Ti/a-C:H multijunction devices with electrical contacts used for current-voltage measurements.

Table 1: Device structure for multiple junction devices. The number of electrical junctions is also indicated. Here MSM indicates metal-semiconductor-metal structures, MIM indicates metal-insulator-metal structures, M-S indicates metal-semiconductor junctions and M-I indicates metal-insulator junctions.

Samples	MSM Structures	MIM Structures	M-S Junctions	M-I Junctions	Total Junctions
C-1	1, Al/Si/Cu	1, Cu/a-C:H/Cu	2, Al/Si and Si/Cu	2, Cu/a-C:H and a-C:H/Al	4
C-2	1, Al/Si/Cu	2, Cu/a-C:H/Cu Cu/a-C:H/Al	2, Al/Si and Si/Cu	4, Cu/a-C:H, a-C:H/Cu, Cu/a-C:H and a-C:H/Al	6
C-3	1, Al/Si/Cu	3, Cu/a-C:H/Cu Cu/a-C:H/Cu Cu/a-C:H/Al	2, Al/Si and Si/Cu	6, Cu/a-C:H, a-C:H/Cu, Cu/a-C:H, a-C:H/Cu, Cu/a-C:H and a-C:H/Al	8
C-4	1, Al/Si/Cu	4, Cu/a-C:H/Cu Cu/a-C:H/Cu Cu/a-C:H/Cu Cu/a-C:H/Al	2, Al/Si and Si/Cu	8, Cu/a-C:H, a-C:H/Cu, Cu/a-C:H, a-C:H/Cu, Cu/a-C:H, a-C:H/Cu, Cu/a-C:H and a-C:H/Al	10
T-1	1, Al/Si/Ti	1, Ti/a-C:H/Ti	2, Al/Si and Si/Ti	2, Ti/a-C:H and a-C:H/Al	4
T-2	1, Al/Si/Ti	2, Ti/a-C:H/Ti Ti/a-C:H/Al	2, Al/Si and Si/Ti	4, Ti/a-C:H, a-C:H/Ti, Ti/a-C:H and a-C:H/Al	6
T-3	1, Al/Si/Ti	3, Ti/a-C:H/Ti Ti/a-C:H/Ti Ti/a-C:H/Al	2, Al/Si and Si/Ti	6, Ti/a-C:H, a-C:H/Ti, Ti/a-C:H, a-C:H/Ti, Ti/a-C:H and a-C:H/Al	8
T-4	1, Al/Si/Ti	4, Ti/a-C:H/Ti Ti/a-C:H/Ti Ti/a-C:H/Ti Ti/a-C:H/Al	2, Al/Si and Si/Ti	8, Ti/a-C:H, a-C:H/Ti, Ti/a-C:H, a-C:H/Ti, Ti/a-C:H, a-C:H/Ti, Ti/a-C:H and a-C:H/Al	10

3. Results and Discussion

In general thin a-C:H films show a disordered amorphous structure; in this study we have employed simple metal/a-C:H bilayer and multilayer approaches to transform from an amorphous to nanostructure morphology of the a-C:H films. Figure 2 shows the scanning electron microscope images of representative Cu/a-C:H and Ti/a-C:H multilayer samples having one bilayer. Both of these samples are found to show the formation of carbon nanostructures. In the case of the Cu/a-C:H bilayer sample, the small carbon nanoparticles are found to adhere to one another forming an agglomerated fibrous carbon network. However, in the Ti/a-C:H bilayer sample, the formation of carbon nanospheres is observed and because of their higher packing

density, these carbon nanospheres are found to bind together forming carbon derived clusters of nanospheres. The presence of thin metallic Cu or Ti layers below the a-C:H film therefore plays an important role in transforming the morphology of a-C:H overlayer. The Cu and Ti layers are found to assist in transforming the film's amorphous morphology to one with a nanostructure morphology of the a-C:H films and the observed nanostructured morphology greatly influences the functional properties of a-C:H films.

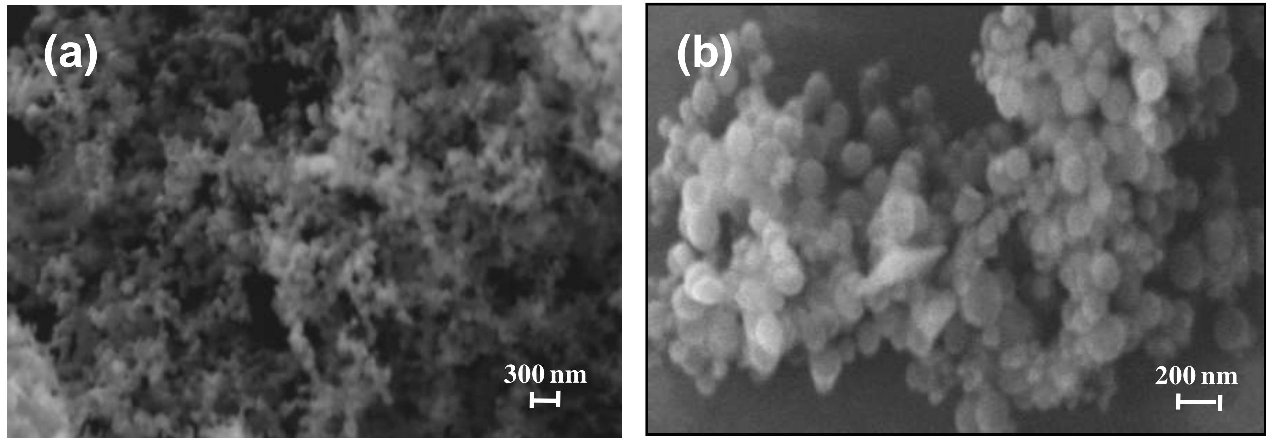

Figure 2: Scanning electron microscopy images of (a) Cu/a-C:H and (b) Ti/a-C:H multilayer structures having one bilayer.

The variation of the residual stress with number of bilayers for the multilayer structures is shown in Figure 3. Compared with single layer DLC films, these multilayer samples show low residual stress due to the presence of alternating metal and a-C:H layers, which allow for stress relaxation in the overall structure. The residual stress is found to increase with the increasing number of bilayers from one to three but decreases again for the multilayer having four bilayers. Among Cu/a-C:H and Ti/a-C:H multilayer structures, the Cu/a-C:H multilayer structures consistently show lower residual stress when compared to the Ti containing structures. This is attributed to the fact that Cu does not readily form a carbide and hence, may avoid the formation of a mixed layer at the interface. By contrast, Ti has strong affinity with carbon and readily forms a carbide layer, which leads to the formation of mixed layers at the interfaces that enhance interfacial mismatch and higher stress.

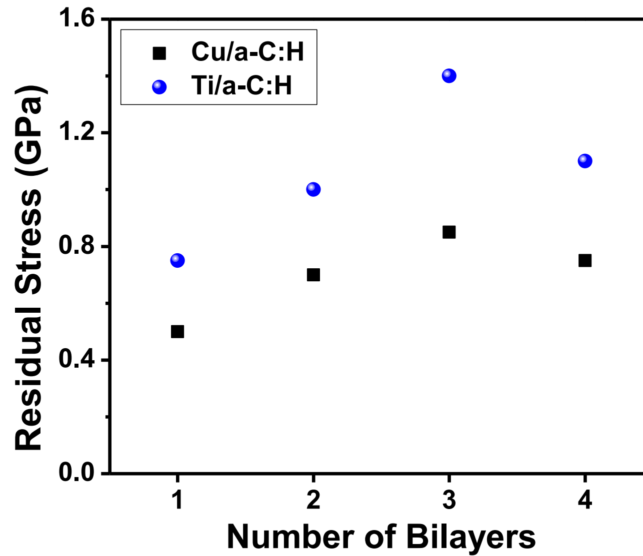

Figure 3: Variation of residual stress with number of bilayers for Cu/a-C:H (■) and Ti/a-C:H (●) multilayer structures.

Using TOF-SIMS, the depth profile of the constituent atoms from representative Cu and Ti containing samples is shown in Figure 4a and 4b. During the growth of a-C:H films, energetic carbon ions hit the surface of the substrate and create local areas of heating which results in the diffusion of C atoms into the Si substrate; this can lead to an interfacial mismatch. Using TOF-SIMS, we have investigated not only the depth profile of the constituent atoms but also examined their interdiffusion. As Cu was the first layer deposited on the substrate, Cu atoms can be seen (Figure 4a) to have diffused into the Si substrate. Atoms of C and H are also seen to diffuse with H diffusing furthest into the Si substrate; this is attributed to its low atomic mass. Since the first interlayer of Cu acts as a barrier, the diffusion of C atoms into Si is reduced. We believe that due to relatively small atom interdiffusion these Cu/a-C:H multilayer structures exhibit low stress, below 1 GPa. Sample T-4 shows the diffusion of C, H and Ti atoms into Si where the diffusion of C atoms into the substrate is found to be comparatively higher in sample T-4 than in sample C-4; this results in comparatively higher measured stress in sample T-4.

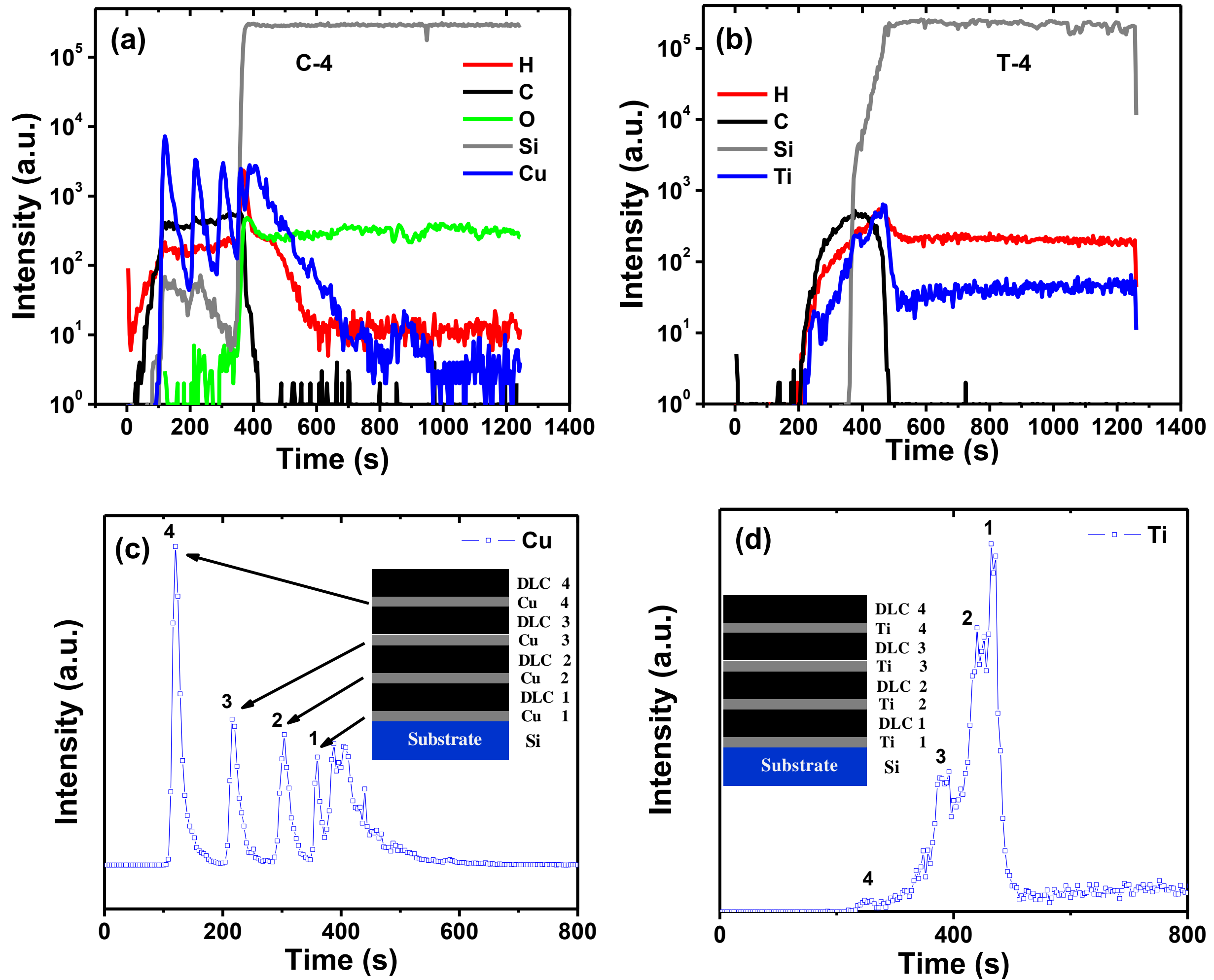

Figure 4: TOF-SIMS depth profile of (a) sample C-4, (b) sample T-4, (c) Cu from C-4 and (d) Ti from T-4.

Figures 4c and 4d show the depth profile of Cu and Ti layers with sputtering time, and the insets show a schematic of the structures investigated from representative samples. Figure 4c clearly reveals the presence of four peaks corresponding to the presence of Cu layers at discrete intervals. Since Cu does not form a carbide, little bonding between the C and Cu atoms occurs. This results in sputtering of the Cu target during the deposition of each Cu layer despite the presence of some carbon atoms, which covers the Cu sputtering target before the deposition of the second, third and fourth Cu layer. The intensity of the Cu peak, which is the lowest for the peak labelled 1, progressively increases for peaks 2, 3 and then 4. The primary ions fall on the sample from the top, and first encounter the fourth a-C:H layer followed by the fourth Cu layer. Only one a-C:H layer was present before the fourth Cu layer which explains the high intensity signal from the Cu

atoms. However, deeper into the sample the signal from the C and H atoms starts to dominate and this leads to a continuous reduction in the intensity of the Cu peaks (peaks labelled 3, 2 and 1). By contrast, the intensity of the Ti peak increases on going inward into the sample as Ti makes a strong bond with C atoms. Before deposition of the first Ti layer (peak labelled 1), no a-C:H layer was grown, and hence, no carbon is present in the Ti layer. Because of this the highest intensity Ti peak is obtained for the Ti peak labelled 1. However, before deposition of the second Ti layer (peak 2), a single a-C:H layer was deposited. As a result, some carbon is also deposited onto the target that leads to comparatively less sputtering from the Ti target owing to strong bonding of TiC. The process continues and the intensity of Ti peak is successively reduced from top to bottom (from peak 1 to 4) in the sample.

Figures 5a–5d show the electrical current – voltage characteristics, presented in a variety of different forms including log I versus $V^{1/2}$ and log I versus $V^{1/4}$ curves of various Cu containing multijunction devices. The corresponding characteristics of Ti/a-C:H multijunction devices are shown in Figures 6a–6d. The I-V curves of these multijunction devices are found to be nonlinear however in both devices the behaviour of the current during positive voltage and during negative voltage are found to be symmetrical. The current in these metal/a-C:H devices is found to be higher than the usual single layer a-C:H devices. This can be due to the metal-induced formation of nanostructured morphology within the a-C:H layer in metal/a-C:H devices, which further enhances the electrical transport. In addition, specifically in case of Cu/a-C:H bilayer device, the deposition of a-C:H on Cu containing Si may lead to the formation of higher sp^2 bonding given the fact that metal promotes sp^2 bonding leading to the presence of an increased graphitic phase. Thus, the formation of relative higher sp^2 bonding content in Cu/a-C:H bilayer device, in contrast with the Ti/a-C:H devices, may be one of the reasons for the increased current in Cu/a-C:H devices.

We have further analysed the electrical characteristics of Cu/a-C:H and Ti/a-C:H multijunction devices in depth. The Cu/a-C:H multijunction devices show very low current flowing below a certain voltage, see below, referred to as the turn-on voltage. This turn-on voltage is found to be a function of the number of junctions with sample C-1 having only four junctions,

showing the highest current and lowest turn-on voltage (between 1 and 1.5 V). Sample C-4 with a total of ten junctions in series exhibits the lowest current and highest turn-on voltage about 3 V. The I-V curves of Ti/a-C:H multijunction devices show a similar behaviour below the turn-on voltage, with sample T-1 having four junctions, exhibiting the lowest turn-on voltage and sample T-4 (ten junctions) has the highest turn-on voltage (~ 4 V).

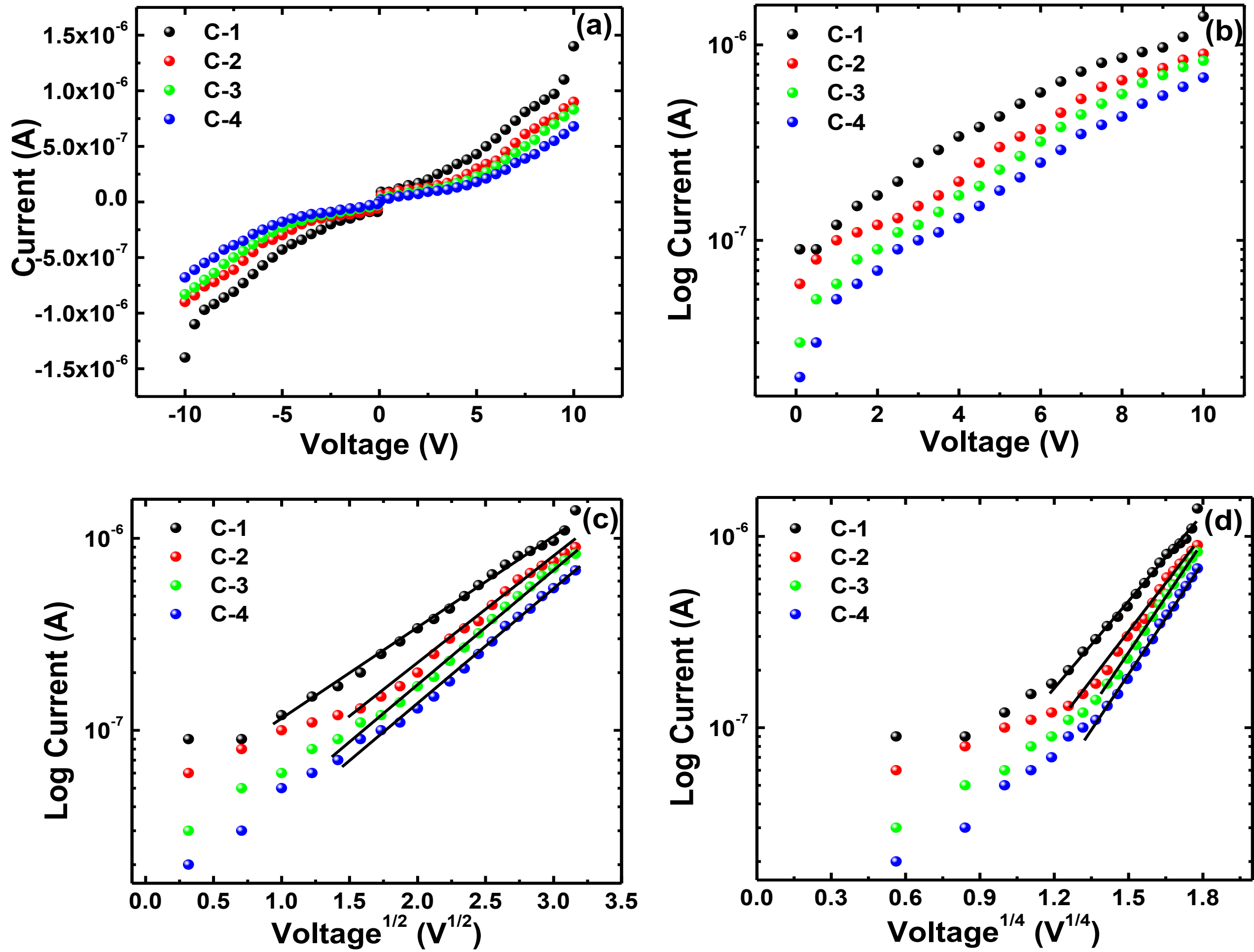

Figure 5: Electrical current-voltage characteristics of Cu/a-C:H multijunction devices presented in different format (a) I versus V, (b) log I versus V, (c) log I versus $V^{1/2}$ and (d) log I versus $V^{1/4}$.

Comparing the Ti/a-C:H and Cu/a-C:H multijunction devices, the Cu/a-C:H devices exhibit a lower turn-on voltage and higher current, which is attributed to the inclusion of Cu layers that help to enhance sp^2 bonding. However, the presence of Ti helps to maintain a hard diamond-like sp^3 bonding though accompanied by higher interfacial stress. In addition, the optical Tauc band gap

in Cu/a-C:H devices is found to be lower than that of Ti/a-C:H devices. The Tauc band gap in samples C-1G, C2-G, C3-G and C4-G (T-1G, T2-G, T3-G and T4-G) deposited on Corning 7059 glass is found to be 1.35 eV, 1.47 eV, 1.7 eV and 1.6 eV (2.1 eV, 2.23 eV, 2.33 eV and 2.2 eV), respectively. The lower Tauc gap will lead to a lower mobility gap which will improve transport explaining why Cu/a-C:H devices showed higher electrical transport than Ti/a-C:H devices.

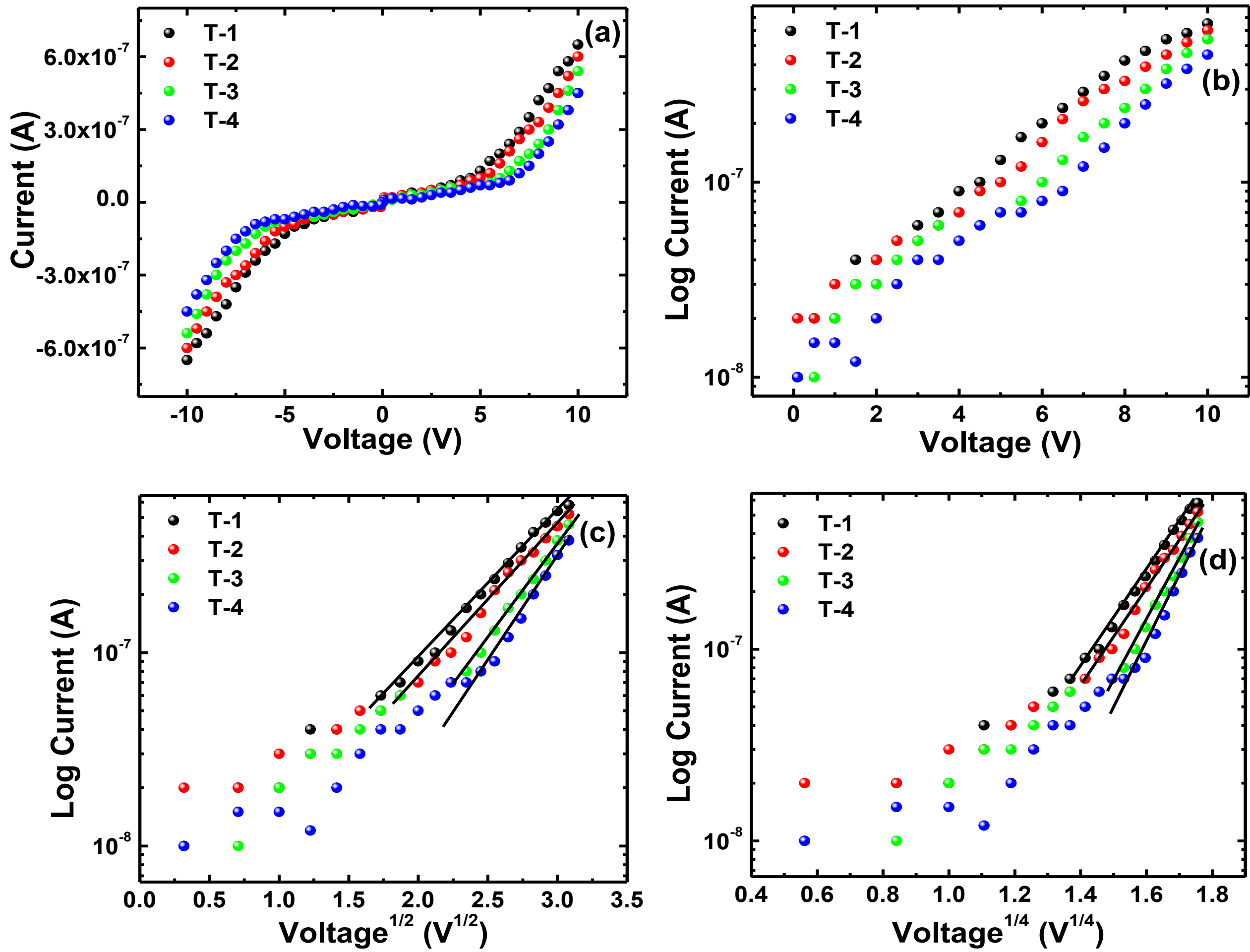

Figure 6: Electrical current-voltage characteristics of Ti/a-C:H multijunction devices presented in different format (a) I versus V, (b) log I versus V, (c) log I versus $V^{1/2}$ and (d) log I versus $V^{1/4}$.

The electrical transport can be analysed by examination of the electrical characteristics based on log I versus V curves for Cu/a-C:H and Ti/a-C:H multijunction devices (Figures 5b and 6b). These curves reveal ohmic conduction in the low voltage region but deviate from linear behaviour at higher voltages. In order to investigate the conduction mechanism, the curves are plotted as log I versus $V^{1/2}$ and log I versus $V^{1/4}$ to distinguish between the Schottky, Poole-

Frenkel or hopping (near the Fermi level) conduction mechanisms. The best fit to the data was obtained when plotting log I versus $V^{1/2}$, where a linear behaviour at moderate and higher voltages is seen. It is proposed that at moderate voltages the Schottky mechanism is the most plausible explanation for conduction, however, at higher voltage transport by the Poole-Frenkel conduction mechanism is the most likely. Chiu *et al.* [18] observed a similar transition in conduction mechanism in amorphous Ta_2O_5 thin films with a Schottky conduction mechanism at low voltages and Poole-Frenkel conduction at high voltages. Khan *et al*. [19] also observed a Poole-Frenkel conduction in low mass ion (boron, carbon and nitrogen) implanted a-C:H films, where the ion implantation helped in the local conversation of sp^3 to sp^2 carbon. Miyajima *et al.* [15, 20] have also observed totally symmetric I-V curves for tetrahedral amorphous carbon based diodes and nitrogenated amorphous carbon films, and proposed Poole-Frenkel conduction mechanism played the controlling role at higher voltages.

4. Conclusion

In conclusion, Cu/a-C:H and Ti/a-C:H multilayer hybrid thin films were prepared and devices fabricated, and studied for their interfacial, structural properties and electrical characteristics. The current and conductivity was found to be higher in these multijunction/multilayer devices than conventional a-C:H based single junction layer devices. A significant difference is found depending on whether the metal chosen is carbide or non-carbide forming with higher current, lower stresses and better adhesion consistently found with the non-carbide forming metal, copper. The present study will be useful to understand the device physics of metal and carbon based multi-junction devices.

Acknowledgements

The authors are grateful to the Director, NPL New Delhi for his kind support. Thanks are also due to Dr. Chetna Dhand, Ms. Kalpana Lodhi, Dr. N. Karar, and Dr. O. S. Panwar for their help.

References

[1] L. Britnell, R. Gorbachev, R. Jalil, B. Belle, F. Schedin, M. Katsnelson, L. Eaves, S. Morozov, A. Mayorov, N. Peres, A. Neto, J. Leist, A. Geim, L. Ponomarenko and K. Novoselov, Nano Letters 12 (2012) 1707-1710 .

[2] T. Georgiou, R. Jalil, B. Belle, L. Britnell, R. Gorbachev, S. Morozov, Y. Kim, A. Gholinia, S. Haigh, O. Makarovsky, L. Eaves, L. Ponomarenko, A. Geim, K. Novoselov, A. Mishchenko, Nature Nanotech. 8 (2013) 100-103.

[3] M. U. Manzoor, C. L. Tuinea-Bobe, F. McKavanagh, C. P. Byrne, D. Dixon, P. D. Maguire, P. Lemoine, J. Phys D Appl. Phys. 44 (2011) 245301.

[4] J.-M. Ting and W.-Y. Wu, Surface Coat. Technol. 231 (2013) 2-5.

[5] N. Dwivedi, S. Kumar, H. K. Malik J. Appl. Phys. 112 (2012) 023518.

[6] S. R. P. Silva, J. D. Carey, Diam. Relat. Mater. 12 (2003) 151-158.

[7] C. Godet, J. P. Kleider, J. Mater. Sci. Mater. Electron. 17 (2006) 413-426.

[8] N. Dwivedi, S. Kumar, C. M. S. Rauthan, O. S. Panwar, Plasma Process. Polym. 8 (2011) 100-107.

[9] N. Dwivedi, S. Kumar, J. D. Carey, H. K. Malik, Govind, J. Appl. Phys. 112 (2012) 113706.

[10] N. Dwivedi, S. Kumar, R. K. Tripathi, J. D. Carey, H. K. Malik, M. K. Dalai ACS Appl. Mater. Interfaces 4 (2012) 5309-5316.

[11] N. Dwivedi, S. Kumar, J. D. Carey, R. K. Tripathi, H. K. Malik, M. K. Dalai, ACS Appl. Mater. Interfaces 5 (2013) 2725-2732.

[12] N. Dwivedi, S. Kumar, R. K. Tripathi, H. K. Malik, O. S. Panwar, Appl. Phys. A 105 (2011) 417-425.

[13] L. Kumari, S. V. Subramanyam, J. Appl. Phys. 99 (2006) 096107.

[14] A. F. Pacheco, J. M. D.Teresa, R. Cordoba, M. R. Ibarra, Phys. Rev. B 79 (2009) 174204.

[15] Y. Miyajima, S. J. Henley, G. Adamopoulos, V. Stolojan, E. G. Caurel, B. Drevillon, J. M. Shannon, S. R. P. Silva, J. Appl. Phys. 105 (2009) 073521.

[16] L. Hao, Q. Xue, X. Gao, Q. Li, Q. Zheng, K. Yan, J. Appl. Phys. 101 (2007) 053718.

[17] N. Dwivedi, S. Kumar, Ishpal, S. Dayal, Govind, C. M. S. Rauthan, O. S. Panwar, J. Alloys Compnd. 509 (2011) 1285-1293.

[18] F. C. Chiu, J. J. Wang, J. Y. Lee, S. C. Wu, J. Appl. Phys. 81 (1997) 6911-6915.

[19] R. U. A. Khan, J. D. Carey, S. R. P. Silva, B. J. Jones, R. C. Barklie, Phys. Rev. B 63 (2001) 121201.

[20] Y. Miyajima, G. Adamopoulos, S. J. Henley, V. Stolojan, Y. Tison, E. G. Caurel, B. Drevillon, J. M. Shannon, S. R. P. Silva, J. Appl. Phys. 104 (2008) 063701.